A strategy to elaborate forest fire spread models for management tools including a computer time-saving algorithm

A STRATEGY TO ELABORATE FOREST FIRE SPREAD MODELS FOR MANAGEMENT TOOLS INCLUDING A COMPUTER TIME SAVING ALGORITHM

A. Simeoni, P.A. Santoni and J.H. Balbi

SPE – CNRS UMR 6134, Campus Grossetti, Università di Corsica, BP 52

20250 Corti, Corsica, France – e-mail: simeoni@univ-corse.fr

Abstract

This paper is devoted to the presentation of a global modelling approach concerning the elaboration of simple forest fire spread semi-physical models to be integrated in operational management tools. The purpose of such models is to represent efficiently the fire behaviour with low calculation times. In a previous study, a semi-physical model was developed which represents correctly the fire spread in a pine needle bed under combined slope and low wind conditions. Then, a multiphase approach was used to improve it theoretically in order to take into account the increasing wind influence. The simulation time remained higher than the real-time, however. Hence, a time saving algorithm was developed which solely solves the semi-physical model in the fire vicinity while providing accurate predictions. This algorithm is presented here as well as its validation thanks to experiments conducted across pine needle fuel beds. This approach represents the last step of the proposed strategy to elaborate forest fire spread models for management tools, which starts from a complete physical model to reach a discrete model to be integrated into a simulator.

Keywords: Fire spread modelling, fire simulator, multiphase model, semi-physical model, diffusion-reaction.

1. Introduction

Forest fire spread modelling deals with several different approaches. Following the classification of Weber [1], one can define three kinds of modelling. The simplest models are the statistical ones which make no attempt to involve physical mechanisms [2]. Otherwise, the empirical models [3] are based upon the conservation of energy but they do not distinguish the modes of heat transfer. Finally, the physical models differentiate among the various kinds of heat transfer in order to predict the fire behaviour [4]. Among them, the multiphase modelling, which takes into account the detailed physical phenomena involved in fire spread, represents the most complete approach that has been developed so far [5].

The aim of our research team is to create an operational management tool which is able to describe the spread of a forest fire in order to help fire fighters to make the appropriate decisions. This kind of simulator necessitates simple and robust models which are able to provide information on the fire spread, within a given margin of error and with a short calculation time. Among the different tools which have been developed so far, the greater part, like BEHAVE [6] or FARSITE [7], are based upon the Rothermel's model [3] which has the disadvantage of being empirical, one-dimensional and steady. Conversely, on the other hand, the FIRETEC model [8], which is based on more physical considerations like combustion modelling and the fluid mechanical governing equations, is inappropriate at the present time to be used in a simulator due to an expensive calculation time. In the current paper we propose an alternative way. To this end, we have developed an unsteady two-dimensional model of fire spread across a fuel bed [9]. This model has not been tested at actual forest fire scale however, and remained only validated at laboratory scale.

This approach was inspired by the diffusion-reaction equation and allowed us to determine, from a single equation, the main characteristics of a laboratory-scale litter fire under both slope and low wind conditions [10,11]. It can be classified as semi-physical. Indeed, the main heat transfers mechanisms are differentiated in this formulation and the model's parameters, which are fuel dependent, are obtained from the fire dynamic. In this last model, we assumed that radiation was the prevailing heat transfer involved in fire spread. Nevertheless, it was unable to predict the fire behaviour for increasing wind velocity. In order to improve it a theoretical study has been conducted based on the multiphase approach [12] which has proved the necessity to add an advection term in the semi-physical model. The calculation time of this last model was higher than the real-time which prevents it from being integrated in a simulator, however.

The aim of this paper is twofold: on the one hand, we will propose an algorithm to evaluate the solution of the semi-physical model solely in the fire front vicinity, which allows a short calculation time while providing simulated results within acceptable margins of error. This algorithm will be tested thanks to experiments conducted across pine needles fuel beds at laboratory scale and under varying conditions (slope, wind and fuel load). On the other hand, we will propose the methodology adopted by our research team as a strategy to elaborate forest fire spread models for management tools, which starts from a complete physical model to reach a discrete model to be integrated into such tools. Indeed, this multiphase approach can be considered as a powerful way of improving or elaborating fire spread models.

The following section presents the multiphase model and its reduction used to improve our semi-physical model. Then, the improved semi-physical model is detailed in the third section. The time saving algorithm which represents the last step of our modelling strategy is then presented in the fourth section. The fifth section is devoted to the presentation of

the experimental methods that were used to validate the results of the simulations. Finally, in the last section the simulation results of the semi-physical model solved with and without the time saving algorithm are compared in relation to experimental data, and the global modelling strategy is proposed.

2. The multiphase approach

2.1. The complete model

As the bases of this model have already been presented [5], only the essential features of this work are provided here. The aim of this approach is to represent the fire spread medium as a reactive and radiative multiphase one. This medium is defined by the fluid phase and *N* solid phases. Each solid phase consists in a set of particles which possess the same geometry and thermochemical properties. An elementary multiphase volume is defined to carry out averaged properties of both gaseous and solid phases. This last volume should be considered as smaller than the scale of the phenomenon but greater than the size of the particle. The system of averaged equations presented hereafter is obtained from [5]. For the sake of clarity, symbols identifying that the variables are volume averaged have been omitted:

Gas phase:

Mass equation

$$\frac{\partial}{\partial t}\left(\alpha_g \rho_g\right) + \vec{\nabla}.\left(\alpha_g \rho_g \vec{V}_g\right) = \sum_k \left[\dot{M}\right]_{gk} \tag{1}$$

Chemical species equation

$$\frac{\partial}{\partial t}\left(\alpha_g \rho_g Y_g^i\right) + \vec{\nabla}.\left(\alpha_g \rho_g Y_g^i \vec{V}_g\right) + \vec{\nabla}.\left(\alpha_g \rho_g Y_g^i \vec{V}_g^i\right) - \alpha_g \rho_g \dot{\omega}_g^i = \sum_k \left[\dot{M}\right]_{gk} \tag{2}$$

Momentum equation

$$\frac{\partial}{\partial t}\left(\alpha_g \rho_g \vec{V}_g\right) + \vec{\nabla}.\left(\alpha_g \rho_g \vec{V}_g \vec{V}_g\right) - \vec{\nabla}.\left(\alpha_g \overline{\overline{\pi}}_g\right) - \alpha_g \rho_g \vec{g} = \sum_k \left[\dot{M}\vec{V}\right]_{gk} + \sum_k \left[\vec{\Pi}\right]_{gk} \tag{3}$$

Total energy equation

$$\begin{aligned} &\frac{\partial}{\partial t}\left(\alpha_g \rho_g e_g\right) + \vec{\nabla}.\left(\alpha_g \rho_g e_g \vec{V}_g\right) + \vec{\nabla}.\left(\alpha_g \left(\vec{q}_g + \vec{R}_g\right)\right) - \vec{\nabla}.\left(\alpha_g \overline{\overline{\pi}}_g.\vec{V}_g\right) \\ &- \alpha_g \rho_g \vec{g}.\vec{V}_g = \sum_k \left[\dot{M}e\right]_{gk} - \sum_k \left[q\right]_{gk} - \sum_k \left[R\right]_{gk} + \sum_k \left[\vec{\Pi}.\vec{V}\right]_{gk} \end{aligned} \tag{4}$$

Solid Phase (*N* equations, one per *k* phase):

Mass equation

$$\frac{\partial}{\partial t}\left(\alpha_k \rho_k\right) = -\left[\dot{M}\right]_k^{surf} - \left[\dot{M}\right]_k^{pr} \tag{5}$$

Chemical species equation

$$\frac{\partial}{\partial t}\left(\alpha_k \rho_k Y_k^i\right) = -\left[\dot{M}\right]_k^{surf,i} - \left[\Gamma\right]_k^{surf,i} - \left[\dot{M}\right]_k^{pr,i} \tag{6}$$

Total energy equation

$$\frac{\partial}{\partial t}\left(\alpha_k \rho_k e_k\right) = -\left[\dot{M}e\right]_k^{surf} - \left[\dot{M}e\right]_k^{pr} - \left[q\right]_k - \left[R\right]_k + \left[\vec{\Pi}.\vec{V}\right]_k^{pr} \tag{7}$$

It should be noticed that no momentum equation appears in the solid phase because it is assumed that the solid phases are motionless. To close the mathematical problem, interface equations are added, and a radiative equation is included to express the radiative contribution in the equation of energy of the different phases (4) and (7). From this method, different sub-models appear on the right hand side of the previous balance equations that should be determined. These last sub-models and the interface equations as well as the radiative transfer equation are not detailed here for clarity, but the interested reader is referred to [5]. This approach has been reduced in order to propose a method for improvement of semi-physical forest fire spread models. Indeed, the three-dimensional model presented here, which takes into account the finest mechanisms involved in fire behaviour, is not appropriate at the present time to be integrated in fire

spread simulators since it needs considerable calculation time. To avoid this disadvantage, we have developed a two-dimensional semi-physical model, based on a single thermal balance, as well as a method to improve it. This method involves the reduction of the complete multiphase model and will be presented hereafter. It leads to a simplified multiphase formulation which nears our semi-physical one (while keeping significant physical information) and which can be used to improve it.

2.2. The reduced model

The multiphase model reduction has been carried out in three steps. Firstly, as the semi-physical model is two-dimensional, we reduced the three dimensional multiphase set of equations to two dimensions by applying an averaging procedure on the z-dimension along δ, the height of the fuel layer, (cf. Fig. 1).

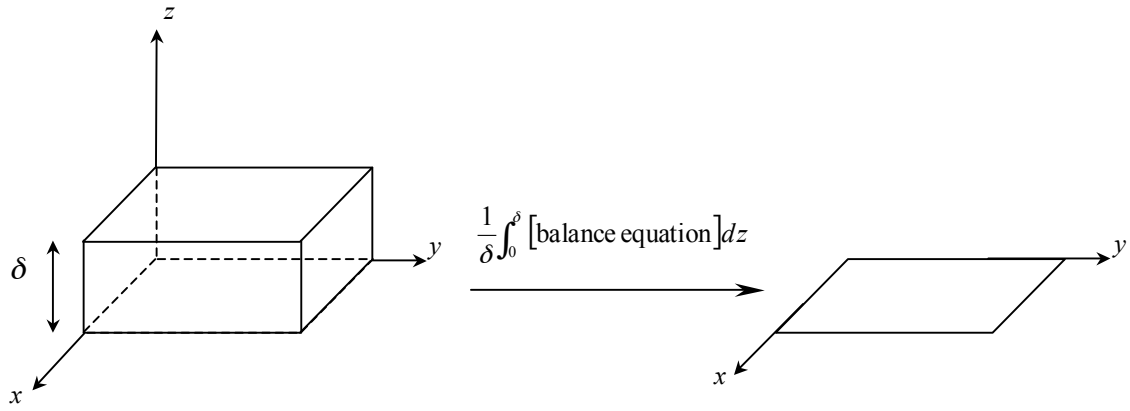

Fig. 1. The two dimensional reduction procedure

For clarity, no symbol representing that the variables are averaged will be added in the following equation. Secondly, since our semi-physical models is characterised by a single energy conservation equation, the thermal balances of the multiphase model (equations 4 and 7) have been reduced to one single equation by means of the thermal equilibrium assumption. Finally, the

resulting conservation equation of energy has been expressed in terms of temperature by using the previous set of reduced equations. After making calculations and setting some hypothesis of reduction, we obtained the following equation in which pressure, stress, gravity and conduction contributions are neglected and a single solid phase is considered [12]:

$$\left(\alpha_g \rho_g C_{p,g} + \alpha_k \rho_k C_{p,k}\right) \frac{\partial T}{\partial t} + \alpha_g \rho_g C_{p,g} \vec{V}_{g,s} . \vec{\nabla}_s T + \vec{\nabla}_s . \left(\alpha_g \vec{R}_{g,s}\right) + \frac{\left[\alpha_g R_{g,z}\right]_0^\delta}{\delta} = -\left[\dot{M}\right]_k^{pr} L^{pr} - \left[\dot{M}\right]_k^{surf} \Delta H^{surf} - \sum_i \alpha_g \rho_g \dot{\omega}_i h_g^i \quad (8)$$

This equation represents the mean mechanisms of propagation like convection, radiation and reactions. Furthermore, it is expressed in a form that enables resolution through the expression of appropriate sub-models. It should be borne in mind that (8) is only a part of the whole reduced multiphase model which is derived from (1) to (7). This reduced model remains too far from our aim which is to elaborate a simple model which can be used as an operating management tool. It can be considered as a useful tool of improvement of semi-physical models however. Thus, (8) has been compared with the semi-physical model presented hereafter, so as to improve it.

3. The semi-physical modelling

Due to the amount of physical phenomena and state variables involved in fire behaviour, it is necessary to reach our aim, to make some simplifying hypotheses in order to generate a comprehensive and simple model. These hypotheses lead us to combine these physical phenomena and to consider a thermal balance which provides the framework of the model. In order to write it, elementary cells composed of soil and plant matter are defined.

As a whole, these cells are considered to represent a thin, isotropic and homogenous medium equivalent to the litter. The energy transferred from a cell to the surrounding air is considered to be proportional to the difference between the temperature of a cell and the ambient temperature.

Combustion reaction is assumed to occur above a threshold temperature (T_{ig}). Above this threshold, we suppose that the fuel mass decreases exponentially and that the quantity of heat generated per unit fuel mass is constant. The heat transferred between a cell and its neighbouring cells is due to three mechanisms: radiation, convection and conduction. We assumed that these exchanges can be represented by a single equivalent diffusion term, under no slope and no wind condition.

However, due to obvious geometric reasons, a supplementary radiation was considered for upslope and low upwind fires. In order to evaluate it we consider the flame to be a vertical radiant surface, the temperature of which is equal to the temperature of the burning cell located below it. This temperature is given by the model. By using a Stefan-Boltzmann law, we assume that the radiant heat flux is proportional to T^4 and that it prevails over a short distance d (in the calculation performed in this paper, d is equal to the spatial increment value of 0.01 m). From a previous work [10], we established that an unburned cell in the direction of the slope receives an additional radiant heat flux, from a burning cell directly before it, which is proportional to the cosine of the angle θ located between the normal of the front and the direction of the slope:

$$R = P(\phi)\cos(\theta)T^4(x-d,y,t) \tag{9}$$

where $T(x-d,y,t)$ is the temperature of the burning cell located just before the unburned cell under consideration. $P(\phi)$ being a function of the flame tilt angle, the emissivity of the flame, the absorptivity of the fuel and the view factor. It is not reasonable to take all these parameters into consideration in our macroscopic approach. Hence, $P(\phi)$ has been determined based on laboratory fire experiments from an empirical law [11].

For upwind fires, a convective term was added in the model too [12]. Indeed, making the comparison between the equation of the simplified multiphase model (8) with the semi-physical model one, we remarked that both models consider chemical kinetic, radiant and convective heat transfer. The main striking difference between the two formulations consisted in the advection

contribution which was omitted in our model. So, we decided to add an advective term in our formulation to finally obtain the following model of fire spread:

$$\frac{\partial T}{\partial t} + k_v \vec{V}_g . \vec{\nabla} T = -k(T - T_a) + K\Delta T - Q\frac{\partial \sigma_k}{\partial t} + R \qquad (10)$$

$R = 0, \quad \sigma_k = \sigma_{k0} e^{-\gamma(t - t_{ig})}$ for a burning cell

$R = P(\phi)\cos(\theta) T^4(x - d, y, t), \quad \sigma_k = \sigma_{k0}$ for an inert cell ahead of the fire front

$R = 0, \quad \sigma_k = \sigma_{k0}$ for an unburned cell elsewhere

$V_g = V_\infty$ on the whole domain

$T = T_a$ at the boundaries far from the fire

$T(x, y, t = 0) = T_a$ for an unignited cell at time zero

$T(x, y, t = 0) = T_{ig}$ for an ignited cell at time zero

where t_{ig} is the time for which $T = T_{ig}$. The model parameters (k, K, Q and γ) are determined using the experimental temperature measurements over time for a fire spreading in a linear way under no slope and no wind conditions [9]. Due to our approach, these parameters are fuel-dependent and must therefore be identified for each fuel. Thus, the usual fuel descriptors such as mass per unit area, particle size, compactness, physico-chemical properties and moisture content are intrinsically taken into account. $P(\phi)$ has been determined using the following empirical law [11]:

$$P(\phi) = p_0 \sin^4(\phi) \qquad (11)$$

where p_0 is a constant, the value of which will be provided later and ϕ represents the flame tilt angle under upslope and wind-aided conditions. With regard to ϕ, a simple relation was used to determine it: this angle was considered as the composition of the tilt angle due to the slope, (equal directly to the slope angle), and the tilt angle due to the wind effect, (predicted as a composition of the wind velocity and the buoyancy flow velocity, taken both at mid-flame, which was determined in [11]). Concerning the convective term, we assumed as a first step that the maximum wind velocity $\vec{V}_\infty$ can be used in (10) to represent roughly the wind velocity $\vec{V}_g$, present in the whole domain of fire spreading. The coefficient k_v was deduced from the multiphase model, assuming in

addition that the gas is perfect, its specific heat remains constant and the quasi-isobaric approximation is valid [12]. So, we obtain the following relation:

$$k_v = \frac{\alpha_g \rho_a \delta C_{p,g}}{m_{eq}} \cdot \frac{T_a}{T} = k_v^* \cdot \frac{T_a}{T} \tag{12}$$

in which m_{eq} is the surface thermal mass of the semi-physical medium equivalent to the litter and k_v^* is a constant to be determined.

4. The time saving algorithm of calculation

The numerical study of the previous model (10) which was performed firstly on the whole domain of fire spreading revealed that the development of an algorithm was necessary in order to reduce the calculation time however [14]. This involves calculating only in the area surrounding the flame front and not in the entire fire spreading domain. The algorithm allows the development of a calculation domain which is moving with the fire front. It therefore decreases or increases according to the evolution of the solution. Firstly, we will briefly write the discretisation of the semi-physical model, then the algorithm controlling the calculation domain will be presented and subsequently tested.

4.1. The discretisation of the semi-physical model

To manage the discretisation of (10), the Laplacian of *T* at the inner grid nodes is estimated by central finite differences which have a second order accuracy in space. For the advective term an upwind-difference scheme has been used in order to take into account the importance of the gas transfers in the wind direction [13].

The discretisation of (10) on one cell of the computational domain leads to the following differential equation:

$$\frac{dT_{i,j}}{dt} = -k\left(T_{i,j} - T_a\right) - \frac{K}{\Delta x^2}\left(4T_{i,j} - T_{i-1,j} - T_{i+1,j} - T_{i,j-1} - T_{i,j+1}\right) - \frac{k_v}{\Delta x} V_\infty \left(T_{i,j} - T_{i-1,j}\right) - Q\frac{d\sigma_k}{dt} + P(\phi)\cos(\theta)\, T_{i-1,j}^4 \tag{13}$$

where $\frac{d\sigma_k}{dt} = -\gamma\ \sigma_k$ for a burning cell and $\frac{d\sigma_k}{dt} = 0$ elsewhere; $P(\phi) = p_0 \sin^4(\phi)$ for a cell located just ahead of the fire front and $P(\phi) = 0$ elsewhere.

Hence we obtain the following differential system for the whole fire spreading domain:

$$\dot{\Theta} = A\ \Theta + C \tag{14}$$

where A is a matrix which represents the heat transfers, C is the source vector and Θ is the temperature vector (relative to the ambient temperature). In order to reduce the calculation time, the solving of the previous system will be carried out solely in the vicinity of the fire front. Indeed instead of calculating on the whole domain of fire spreading, we will define hereafter a calculation domain which follows the fire front.

4.2. Presentation of the time saving algorithm

We present here the algorithm which will allow the calculation domain to be created. Indeed, the spreading nature of the semi-physical model's solution [9] revealed that, at a particular point in time, only the temperatures surrounding the flame front are of interest. Nevertheless, we must ensure that the numeric solution will not be altered by the running of this algorithm. The basic time saving process is presented in Fig. 2. The main ideas are provided hereafter without going into the finer programming details.

- *Procedure which creates the fire spreading domain:*

This procedure creates a grid for the fire spreading domain which is defined as the whole domain where the fire spread occurs. The fuel complex is divided into an homogeneous rectangular grid, with a mesh size of 0.01 *m*.

- *Procedure used to calculate the solution at each time step:*

This procedure corresponds to the step of the algorithm named “Calculation of the temperature distribution”. The differential equation system (14) has been solved by using the 4th order Runge-Kutta formula. The time step was 0.1 s under no wind conditions and 0.01 *s* under wind-aided conditions.

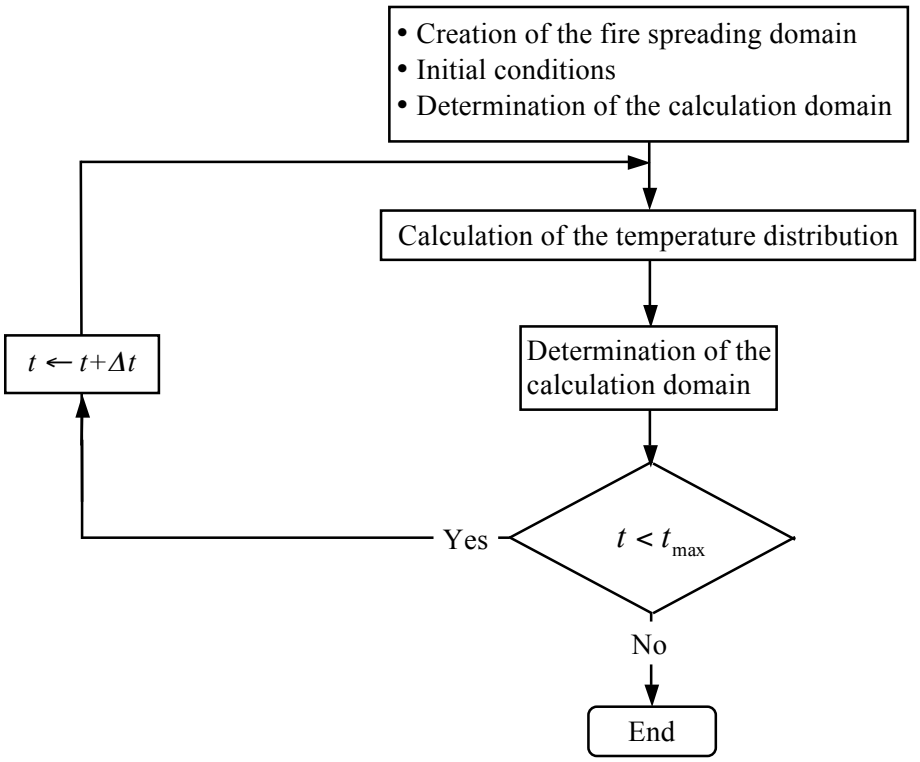

Fig. 2. The time saving algorithm

- *Procedure which manages the calculation domain:*

This procedure corresponds to the step of the algorithm termed "Determination of the calculation domain". It controls the modification of the calculation domain to surround the

fire front. This step will be particularly detailed because it represents the essential of the algorithm's contribution.

As our objective is to create a simulator capable of predicting the spread of forest fires, the areas through which the fire front has already passed and that are located at a certain distance from the front (to be determined) are of little interest as they have already burned. It is therefore not necessary to calculate the temperature for these areas. Conversely, temperature estimates must be made for the fire front area (burning stage) and in the unburned area situated at a certain distance (to be determined) from the fire front and which is subject to heat transfers originating from it (heating stage). The same is not true beyond this area where the temperature is the same as that recorded for the ambient air.

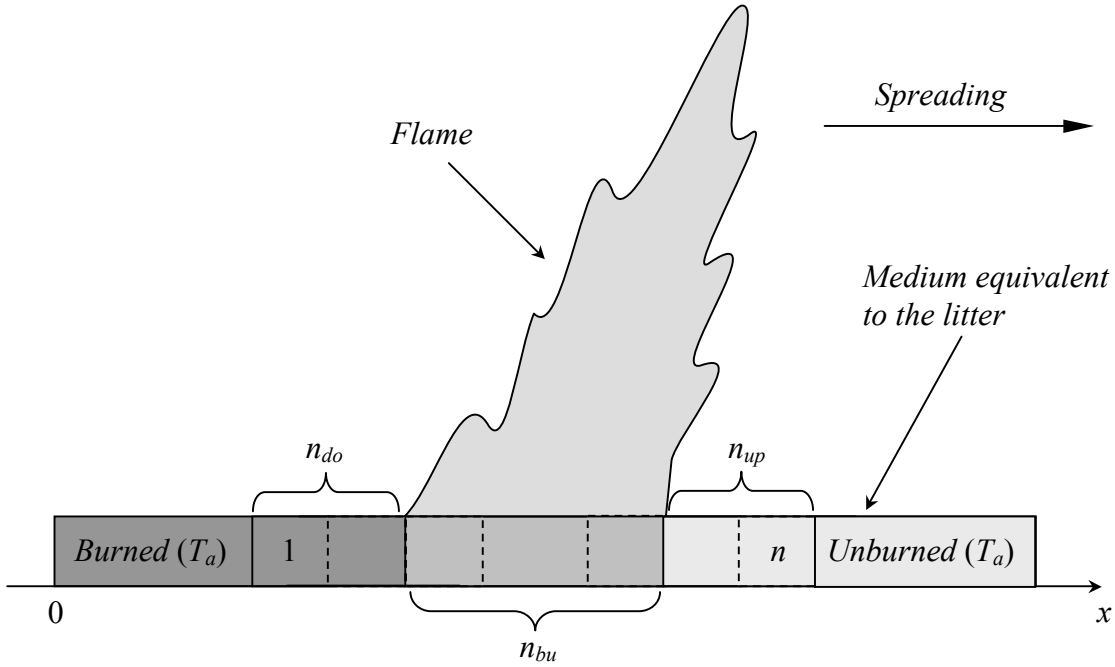

Fig. 3. Sketch of the calculation domain evolution in one dimension

In order to better understand the management of the calculation domain, a simple one-dimensional configuration is depicted hereafter (cf. Fig. 3).

The procedure can be summarized as follows:

- We consider a constant number of cells located in the burned area, downstream

the fire front (n_{do}) and another constant number of cells upstream (n_{up}) in the unburned area. These two numbers can be different.

- The fire front is defined by the burning cells (n_{bu}), i.e. by the cells with a significant energy production term in their thermal balance.
- The part of the domain out of the n cells is considered at the ambient temperature. Thus, we have the total number of cells: $n = n_{do} + n_{bu} + n_{up}$ (cf. Fig. 3). This number does not remain constant in time due to the unsteady nature of the model.
- When the cell located just ahead of the burning area (cell numbered $n_{do} + n_{bu} + 1$) reaches the ignition temperature, this last area increases and the group of n_{up} cells shifts a step in the direction of the spreading.
- When the energy production term of the thermal balance of the cell located at the queue of the burning zone (cell numbered $n_{do} + 1$) becomes negligible, this last zone decreases and the group of n_{do} cells shifts a step forward.

At this point, we have to manage the compromise between the accuracy of the numerical prediction provided by the solving algorithm and the quickness of the calculation. To this end, we have to adjust the criterion that defines the burning zone as well as to establish the convenient pair of cell numbers (n_{do},n_{up}) that allow us to reach this compromise. In order to do this study, we will compare the numerical results to data recorded from experimental fires conducted across pine needles fuel beds which will be presented hereafter.

5. Experimental facilities and procedures

Two sets of experimental data obtained from fire spreading across pine needles will be considered. The first one concerns experiments performed at the I.N.R.A. laboratory of

Avignon (France) under windless and both horizontal and upslope conditions. The second one concerns experiments carried out at the I.S.T. of Lisboa under wind and both horizontal and upslope conditions.

5.1. I.N.R.A. experiments

The experimental fires we have considered were conducted on *Pinus pinaster* litter, in a closed room without any air motion. The experiments were performed in order to observe fire spread over sloping surfaces for line-ignition and point-ignition fires. As the experimental method was given in [15] only the most relevant information (that was useful for our validation) is provided here.

5.1.1. Experimental set-up

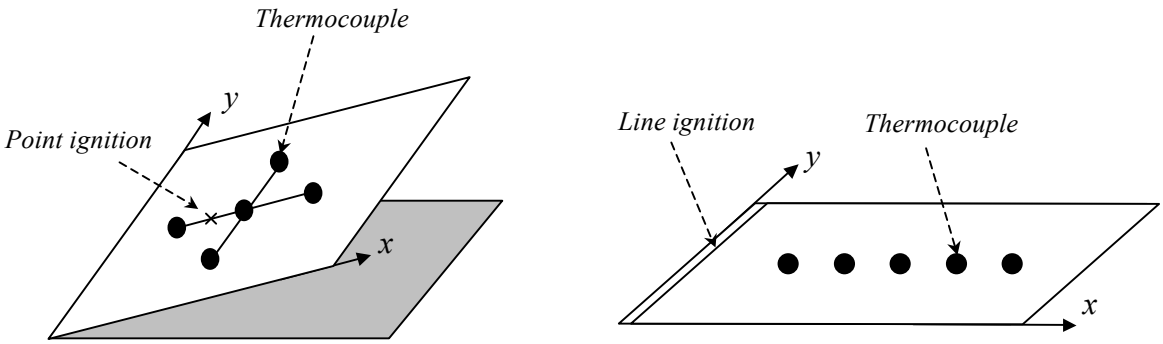

Fig. 4. Experimental devices for a) point ignition fires and b) line ignition fires

For point ignition fires, the experimental apparatus was an aluminium plate of one square meter, protected by sand and inclined in relation to the horizontal plane (cf. Fig. 4a). For line ignition experiments, the combustion table was 170 *cm* long and 59 *cm* wide (cf. Fig. 4b). A porous fuel bed was used, made up of pure oven-dried pine needles spread

as evenly as possible on the total area of the combustion table in order to obtain a homogeneous structure with a fuel load of 0.4 $kg\ m^{-2}$. The needles were conditioned to a moisture content between 1 % and 3 %. The measured surface to volume ratio and density of the needles was 4550 m^{-1} and 680 $kg\ m^{-3}$ respectively.

5.1.2. Experimental runs

The experiments consisted of igniting a point, at the centre of the apparatus for slopeless configuration and shifted on the left for slope configuration. (cf. Fig. 4.a). The experiments were conducted for different slopes ranging from 0° to 30° (10° increments) and three experiments were conducted for each slope. The line ignition fires under horizontal condition consisted in igniting a line using alcohol at one end of the bench. (cf. Fig. 4.b). The resulting spread of the flame across the needles was closely observed with a camera and five K-type (chromel/alumel) thermocouples which were positioned 3 *cm* above the needle bed in order to record temperature. The gauge wire diameter of the thermocouple was 1 *mm*. The fire spread rate was determined for each experiment and the pictures obtained allowed the evolution of flame shape in relation to slope angle to be assessed.

5.2. I.S.T. experiments

5.2.1. Experimental set-up

These experiments were carried out in a dedicated low speed wind tunnel [16] (Fig. 5). They were performed in order to observe wind driven fire across fuel beds of pine needles. Furthermore, the tunnel allows to study both combined wind and slope effects thanks to a sloping fuel tray.

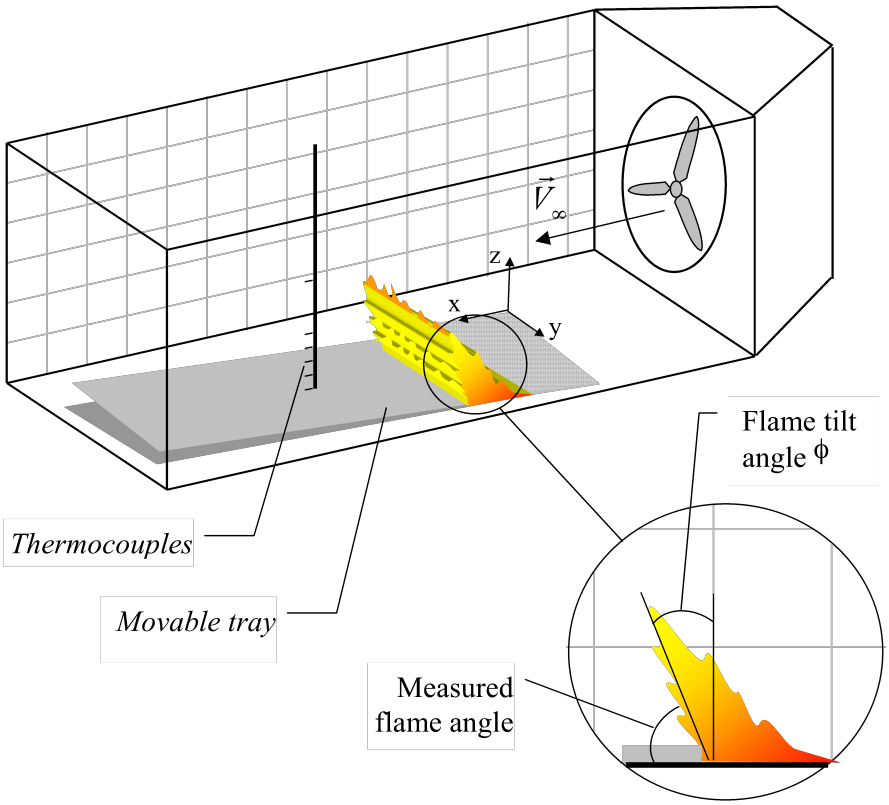

Fig. 5. Experimental wind tunnel

The wind speed values covered the range between 0 to 3 $m\ s^{-1}$ (step 1 $m\ s^{-1}$) for upwind spreading. The movable tray can be set at angles from *0* up to *15°* (step 5°) with upslope orientation. The fuel bed occupies the central part of the tray (*0.70 m* wide). It consists of a layer of *Pinus pinaster* needles, attempting to reproduce a typical layer found in Portuguese stands, with a load of approximately *0.5 kg* m^{-2} on dry basis and a fuel moisture content of (*10 ± 1%*).

5.2.2. Experimental runs

The movable tray is positioned at the required angle and the wind velocity is fixed at the required value. The conditioned pine needles are scattered uniformly on the tray. To ensure a fast and linear ignition, a small amount of alcohol and a flame torch are used. The fuel is

ignited perpendicularly to the flow at the wind tunnel side (Fig. 5). In order to obtain a uniform and established flame propagation, the fuel bed was ignited sufficiently far away from the work section. Three runs are carried out for each set of conditions. The experimental runs are recorded by video. The rate of spread is obtained from the derivative of the curve "flame front position vs. Time". Twenty to thirty images of each experimental run are analysed in order to determine the mean flame angle which is defined as the angle located between the tray and the leading surface of the flame. Temperature measurements are made using K type thermocouples with *250 μm* wire diameter.

6. Results and discussion

In the first place we will deal with the implementation, accuracy and calculation time of this algorithm for both point and line ignition under windless and slopeless condition. Then its capabilities will be examined for upslope and upwind fires. Afterwards a global strategy to elaborate forest fire spread models to be integrated in management tools will be proposed. The method for the identification of the semi physical model's parameters has been presented in [9, 10 and 11]. We obtained the following values for the two sets of experiments:

Table 1. Coefficients of the semi physical model

Experiments	k $\left(s^{-1}\right)$	K $\left(m^2\ s^{-1}\right)$	Q $\left(m^2\ K\ kg^{-1}\right)$	γ $\left(s^{-1}\right)$	p_0 $\left(K^{-3}\ s^{-1}\right)$	k_v^* $\left(K\right)$
I.N.R.A.	71×10^{-3}	31×10^{-6}	3.61×10^{3}	0.19	9.05×10^{-9}	
I.S.T.	97×10^{-3}	14.5×10^{-6}	3.67×10^{3}	0.234	9×10^{-9}	7.5×10^{-3}

6.1. The time saving algorithm: accuracy and calculation time

The algorithm has been tested here by comparing the simulation results with the experimental measurements done at the I.N.R.A. laboratory. The fire front perimeters, the temperature distribution and the fire rate of spread have been chosen for comparison criteria to evaluate its consistency and relevance. At this point, we should recall that the domain of calculation is composed of the numbers of cells n_{do}, n_{bu} and n_{up} of the downstream, inside and upstream fire front sub-domains respectively.

The purpose of this work is not to define an optimal number of cells for each sub-domain but only to show that a limited number of cells can be used to obtain sufficiently accurate results while avoiding heavy and useless calculus. Indeed, the semi-physical model has not been validated at the scale of an actual forest fire, so this topic is meaningless at the present time. To this end, in the following we will present the results of the simulation for the time saving algorithm for a few significant values of the couple (n_{do}, n_{up}). n_{bu} was defined by assuming that a cell pertains to the burning area if the energy which remains to be released at a given time is greater than 10% of its total available energy of combustion.

6.1.1 Accuracy

We must now confirm that the proposed algorithm does not modify the accuracy of the results. To this end, we compared the temperature curves generated without, and with the time saving algorithm for two couples of cell (n_{do}, n_{up}), with the observed one for a line ignition fire (Fig. 7).

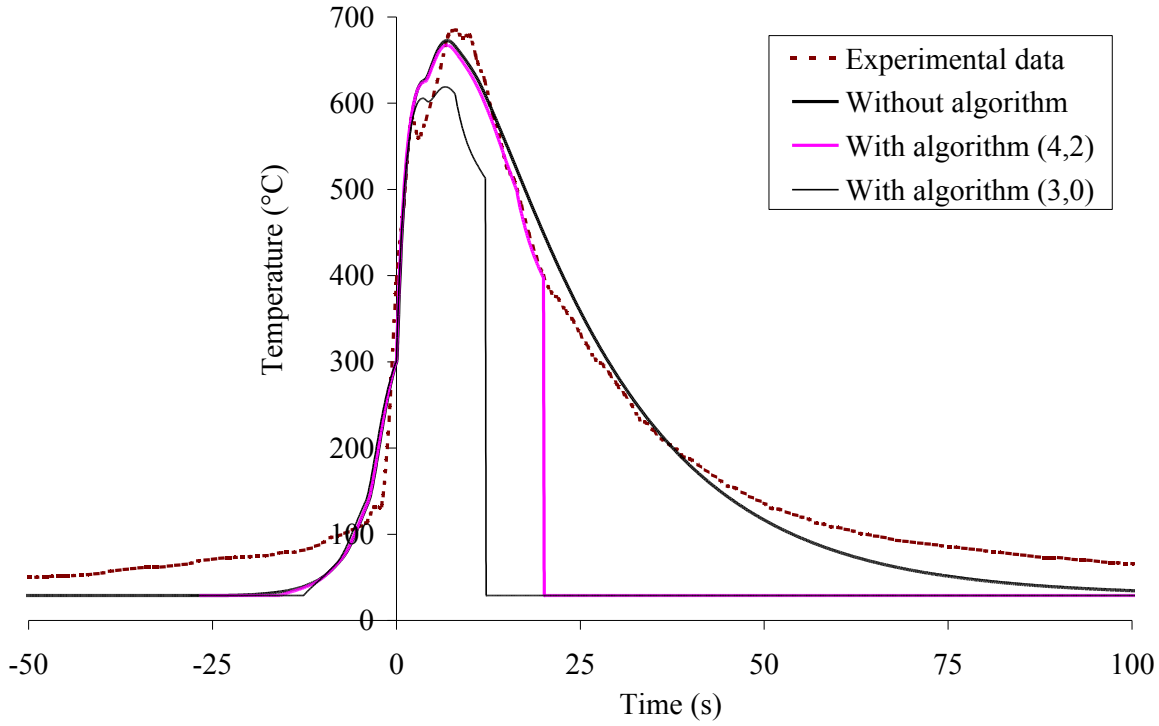

Fig. 7. Observed and predicted with and without the time saving algorithm temperature curves over time at a given point of the domain

It can be seen that the temperature curve generated without the time saving algorithm matches the experimental one. The interested reader can refer to [9] for more details. Moreover the temperature curve generated with the algorithm applied for the couple $(n_{do}, n_{up}) = (4,2)$ is satisfactory too , with the exception of the area in which we cease the calculations. The same is not true of the simulation curve obtained for the couple $(n_{do}, n_{up}) = (3,0)$. A substantial lag in temperature and a poorer evaluation of the maximal value can be observed in this last curve as compared to the two other curves.

With regard to the rates of spread in the steady state, the comparison between the experiments and the simulation points out the same tendency as depicted in Table 2.

Table 2: Spread rate for experiment and simulations

with and without the time saving algorithm

	Rate of spread ($mm.s^{-1}$)	Error (%)
Experiment	3.10	0
Calculation on the whole domain	2.94	5.2
Time saving algorithm with $(n_{do}, n_{up}) = (10,5)$	2.93	5.5
Time saving algorithm with $(n_{do}, n_{up}) = (4,2)$	2.90	6.5
Time saving algorithm with $(n_{do}, n_{up}) = (3,0)$	2.75	11.3

The simulated and observed fire front perimeters for a point ignition at the centre of a one square domain and at a simulation time of *144* seconds are given in Fig. 8 for the couple $(n_{do}, n_{up}) = (4,2)$. In this figure, the small squares denote the position of the experimental flame front. We have superimposed the three sub-domains (burned, burning and unburned) of the algorithm previously defined. We have not provided the perimeter for the calculation on the whole domain since the results were similar to that of the time saving algorithm. We can observe that, for the greatest part, the predicted fire front perimeter (burning zone) coincides with the experiment. The model accurately describes the shape of the front. Furthermore, we can notice that the calculation domain takes on the shape of a ring which develops following the fire front. It should be noticed that the temperature distribution is not provided here for the three sub-domains since it corresponds to the results provided in Fig. 7.

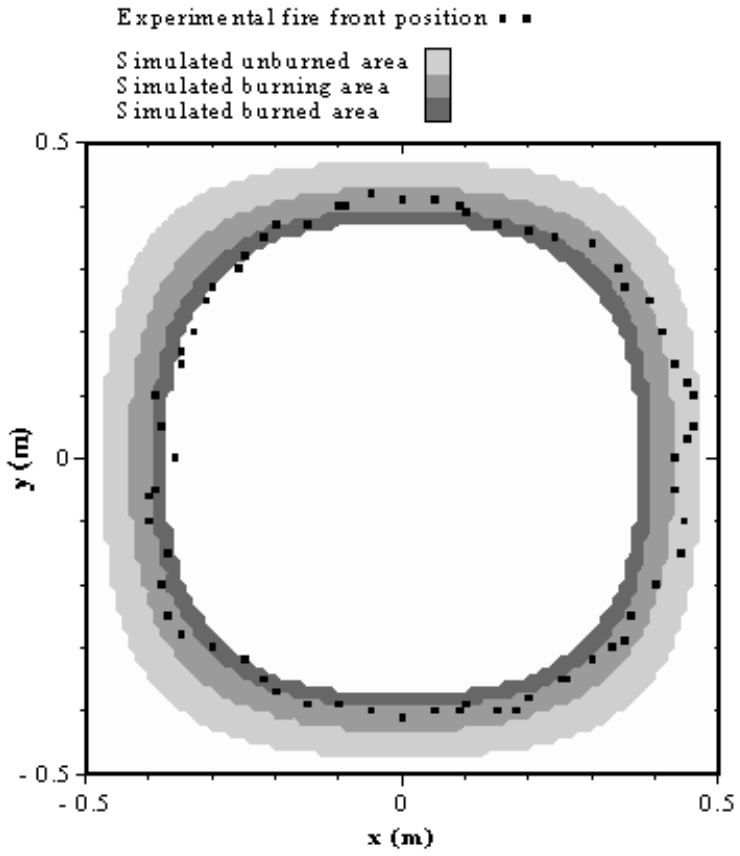

Fig. 8. Observed and predicted with the time saving algorithm fire front perimeters at time 144 *s*

6.1.2. Calculation time

Table 2: Calculation time with and without the time saving algorithm on a Sun Ultra 2 for a simulated spread of 144 seconds after a point-ignition fire.

	CPU time (*s*)
Calculation on the whole domain	114 *s*
Time saving algorithm with $(n_{do}, n_{up}) = (10,5)$	18 *s*
Time saving algorithm with $(n_{do}, n_{up}) = (4,2)$	17 *s*
Time saving algorithm with $(n_{do}, n_{up}) = (3,0)$	17 *s*

We will now present the main advantage of the time saving algorithm: the reduction of the calculation time. To this end, we have included in Table 2 the calculation times for both simulation with and without the time saving algorithm.

In the light of our final goal (which is to develop a forest fire simulator), it can be observed that the simulation time without the time saving algorithm for an actual propagation time of 144 seconds is unacceptable (because it is too close from the real-time). We also note that the reduction in calculation time through the implementation of the time saving algorithm is substantial (6 times). Furthermore, the comparison is made for a simulation domain of only one square meter.

The saving in calculation time would have been even more important had we chosen a greater domain for the same propagation time. Since it depends mainly on the technical characteristics of the computer used, it is preferable to explain the advantage in terms of the number of calculation points, if we are to provide a general formulation. Thus, let N_0 represents the number of points of the calculation domain at a particular time step (defined as the sum of n_{up}, n_{bu} and n_{do} in all directions) and let N_1 represents the number of points of the study domain (which is a square): the saving in number of calculation points is given by $G_1 = N_1/N_0$. When the study domain area is n times greater in terms of number of points $(n\ N_1)$, the saving in number of calculation point is $n\ G_1$. So, the advantage would have been increased with the size of the study domain.

6.2. Further validation simulations for the time saving algorithm

6.2.1. Slope effect (I.N.R.A. experiments)

In this section, we will provide further validation for the time saving algorithm with the couple $(n_{do}, n_{up}) = (4,2)$. We first compare the observed and predicted flame front

perimeters for point ignition fires under 20° (Fig. 9) and 30° (Fig. 10) upslope and windless conditions. We have not provided these results at other times for the 20° upslope, since the agreement is similar to those presented here.

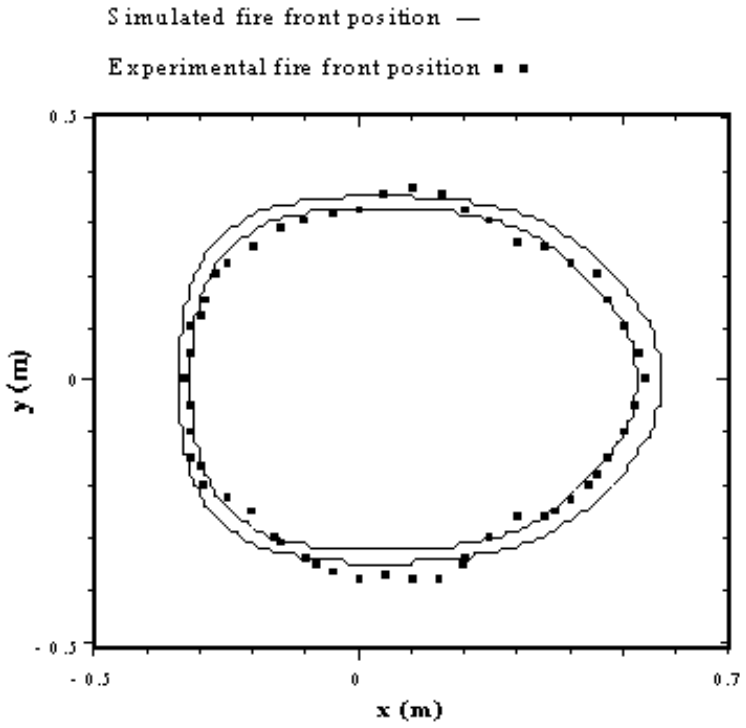

Fig. 9. Comparison between predicted and observed fire front perimeters with a slope of 20° at time 122 *s*

For the fire front perimeters given in Figs. 9 and 10, we superimpose the burning areas generated by the numerical model on the experimental fire perimeters. The model accurately describes the shape of the front for the two slopes. Indeed, a distortion of the fire front is observed in the direction of the slope. Furthermore, an increase in the distortion with both increasing slope (Figs. 9 and 10), and lapse of time for a given slope (Fig. 10), is also described. The unsteady behaviour of the phenomenon is thus performed by the model. Moreover, the fire front spread is well described in the down-slope direction as well as in the other directions. However, we should point out that the deviations in the

experimental fire perimeters are due to the heterogeneity of the needle bed and the heterogeneity of ignition. These conditions are not taken into account in our model and cannot be predicted.

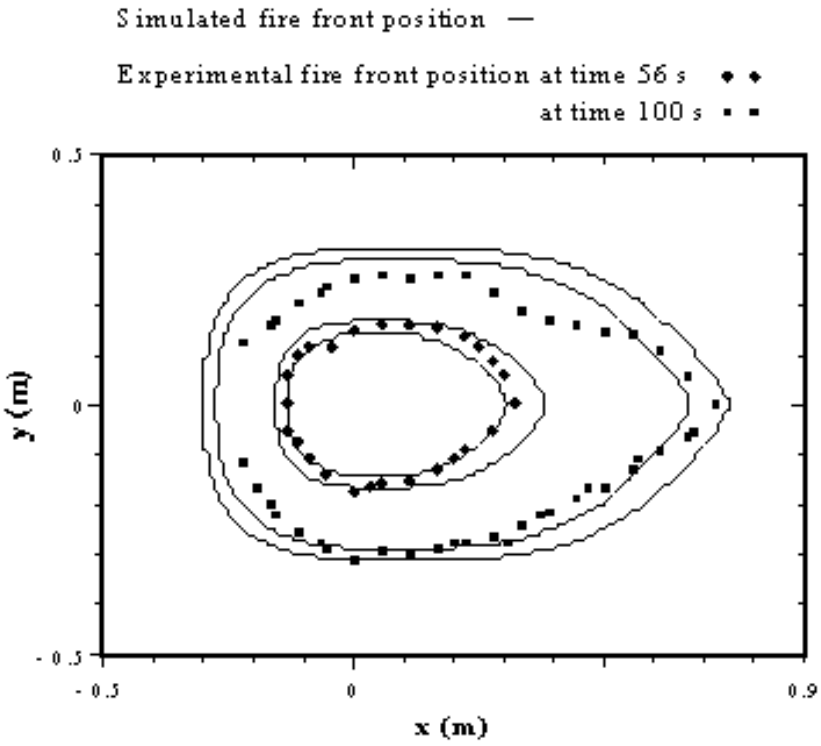

Fig. 10. Comparison between predicted and observed fire front perimeters with a slope of 30° at times 56 *s* and 100 *s*

Concerning Fig. 10, we can note that the fire front perimeter is well predicted at time 56 s, and some discrepancies appear at time 100 s. This behaviour is mainly due to two reasons. The first one deals with the heterogeneity of the fuel bed as stated previously. It can explain the dissymmetry between the two sides of the fire front (also noted in Figs. 8 and 9). The second one concerns the size of the experimental device which is of one square meter. The ignition has been made near from the lower part of the sloping bed to observe the spreading in the up-slope direction. So, at time 100 s, the fire front has already reached the edge of the fuel bed at the bottom of the experimental device, whereas this effect is not

taken into account in simulations. Nevertheless, the main characteristic of the spreading, which is the position of the fire head along time, is well predicted by the model.

Thus, we can affirm that the algorithm allows a good approximation of the fire front perimeter over time and does not disturb the prediction while keeping a similar time saving as previously. Finally, it should be noted that the other aspects of the simulations remain the same as those obtained without the time saving algorithm (rate of fire spread and temperature curves in other directions). So, we do not discuss them here, as we did it in [10] yet.

6.2.2. Both combined slope and wind effect (I.S.T. Experiments)

The time saving algorithm with the couple $(n_{do}, n_{up}) = (4,2)$ has also been kept hereafter since we obtained the same gain in calculation time and the same accuracy (6.5 %) for the rates of spread and temperature distribution as previously. Fig. 11 synthesises the predicted versus observed rates of spread for the whole range of experimental configurations considered. We observe a general agreement between the predicted and observed fire rates of spread for all the slopes considered up to a wind velocity of $2\ m s^{-1}$. The fire rate of spread, which increases with increasing wind or/and slope is predicted.

The difference between the simulated and experimental rates of spread for the higher wind can be explained by comparing the observed and predicted temperature profiles versus time at a given point (cf. Fig. 12). We can observe that the envelope of the simulated result roughly matches the experimental one (excepted the burned area in which we cease the calculation). Before discussing these curves, it should be pointed out that the experimental temperature profiles can only be considered qualitatively, as mentioned in [17]. Indeed, the coupling of the heterogeneity of the fuel spatial distribution with the turbulent nature of the flow involves some scattering and makes an analysis based on the individual temperature traces difficult. Nevertheless, three regimes can be defined:

preheating, peak temperature and cooling zones. Discussion of the peak temperature zone is problematic as the thermocouples do not describe this zone accurately. Indeed, infrared measurements of the same fuel type [18] reveal that the burning area temperature ranges from 1000°C to 1300°C, which is in agreement with our predictions. The cooling in the third zone is beyond the calculation domain and thus is out of interest in our purpose. As for the preheating zone, the model fails to qualitatively describe the increase in fuel bed temperature.

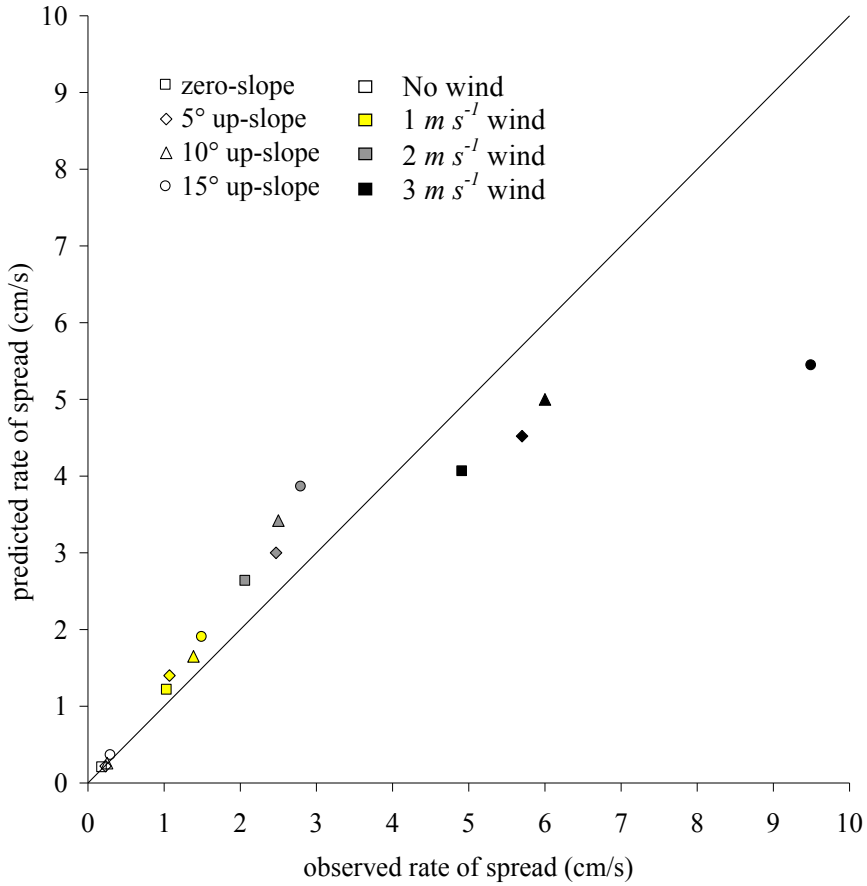

Fig. 11 Predicted versus observed rate of spread for the whole experiments.

The reason for this is to be found in the radiant contribution modelling in (10). Indeed, in order to provide a simple model, we have assumed a short radiant distance effect by considering that radiation prevails in the inert cell ahead of the fire front. It is clear that this

model can be further improved by taking into account the long distance effect of radiant heating ahead of the fire front. Thus, the under-prediction in the rate of spread for wind velocities of 3 $m\,s^{-1}$ is a result of this modelling, and will be improved based on a theoretical multiphase investigation in future studies.

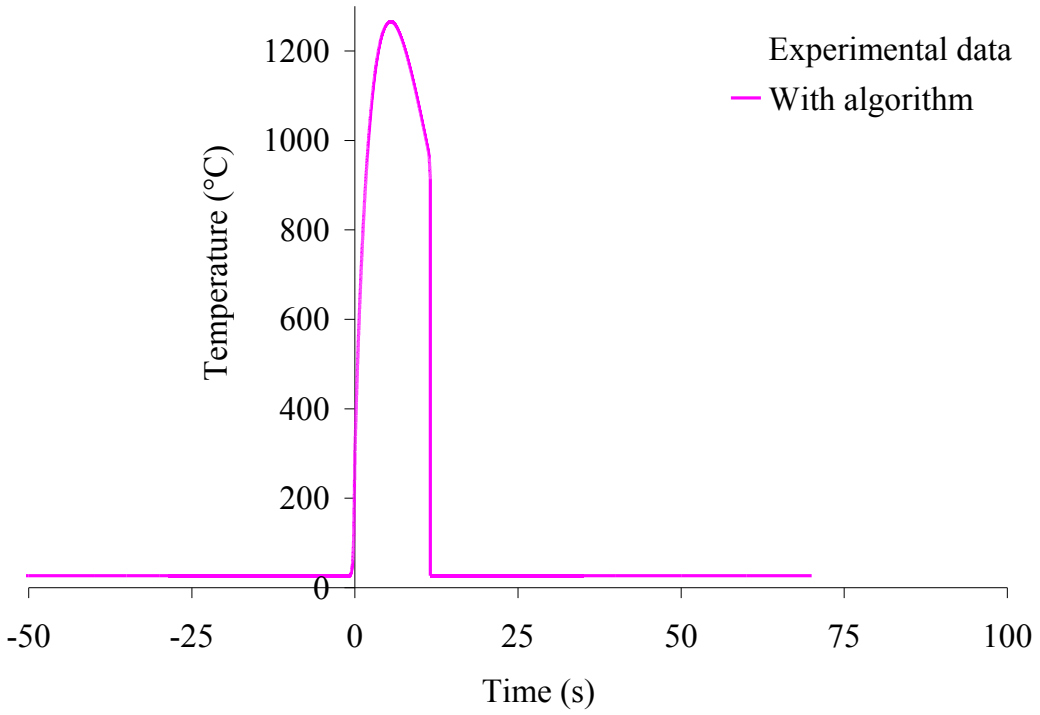

Fig. 12. Experimental and predicted with the time saving algorithm temperature curves for a 10° slope under 3 $m\,s^{-1}$ wind condition

7. Case study of adapting forest fire spread models for management tools

At this point it seems to be convenient to propose the method exposed in this paper as a global strategy to tackle the elaboration of fire spread models to be integrated in management tools. This kind of tool will be dedicated to fire fighters, so its value will reside more in its short calculation time providing the necessary information (rate of fire spread, fire front geometry and temperature field) than in its extreme accuracy. Thus, such

a tool must provide, under real-time, large-scale predictions of the development of a fire line on a vegetation map. Furthermore, the dedicated semi-physical models, whose aim is to take into account the fine mechanisms involved in fire behaviour in a simple manner, require a way of developing simplified equations. This strategy is depicted in Fig. 13. It can be summarised as follows:

- The multiphase modelling approach allows to derive simplified multiphase models based on criteria chosen *a priori* (like thermal equilibrium between solid and gas which leads to a single thermal balance in our case).

- These last models can be used whether to develop semi-physical models or to improve existing ones. For instance as previously presented, our semi-physical model (10) has been improved by adding an advective term after comparison with a suitable simplified multiphase model (8).

- The operational aspect of the strategy concerns the elaboration of appropriate time saving algorithms so as to solve the discrete equations derived from the semi-physical models, for the sake of integrate them in management tools to obtain predictions under real-time.

- The last step in the strategy deals with the confrontation of the simulation results with experiments under varying conditions in order to validate or to invalidate the predictions showing the necessity to improve further the semi-physical model. For example as previously denoted, we will ameliorate in future work the radiant contribution thanks to the multiphase approach.

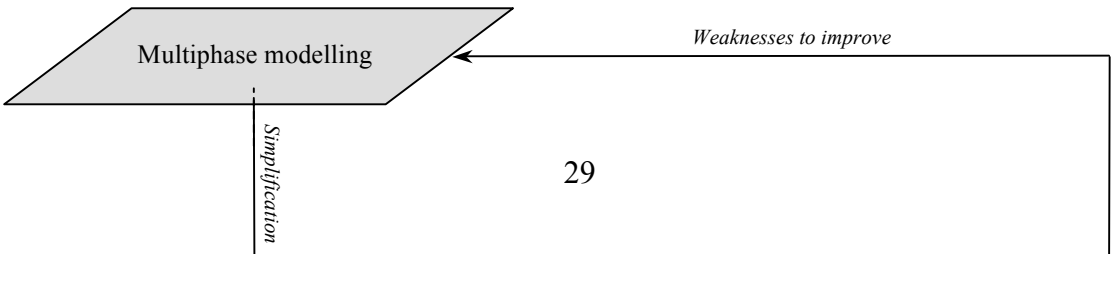

Fig. 13. The modelling strategy

8. Conclusions

The main contributions of this study are:

- The development of an algorithm capable of managing a calculation domain following and surrounding the fire front. The program developed meets our initial objectives. Indeed, the calculation time saved is substantial and the fact that the calculations are performed only in the immediate vicinity of the fire front does not modify the spreading nature of the semi-physical model. The accuracy of the results is not affected either by this algorithm so long as the sub-domains are defined in areas large enough to include the thermal transfers useful for the fire spreading. The calculation time saved is an encouraging result for the development of a forest fire simulator.

- The proposal of a global strategy to elaborate forest fire spread models for management tools offers the advantage to be based on a step by step modelling approach. Indeed, it starts from a strong physical framework (the multiphase model) and allows to elaborate semi-physical models while mastering the simplifying assumptions used to

derive them. Furthermore, it permits a feed back towards the complete multiphase model, in order to take into account other characteristics of the fire behaviour. We intend to do it in future work more specifically for the long-range radiant preheating mechanism which will be included in the present semi-physical model.

In addition, future research will include the simulation of fire spread under complex topographical conditions as well as the achievement of prescribed fires at actual bush fire scale to investigate the behaviour of our semi-physical model at larger scales.

References

[1] Weber, R.O. Modelling fire spread through fuel beds. *Progress in Energy and Combustion Science 17*, 1990, 67-82.

[2] McArthur, A.G. Weather and grassland fire behaviour. (Australian Forest and Timber Bureau Leaflet N° 100, 1966).

[3] Rothermel, R.C. A mathematical model for predicting fire spread in wildland fuels. *USDA, Forest Service Research*. Paper INT-115, 1972.

[4] Albini, F.A. A model for fire spread in wildland fuels by radiation. *Combustion Science and Technology, 42*, 1985, 229-258.

[5] Larini, M., Giroux F., Porterie B., and Loraud J.C. A multiphase formulation for fire propagation in heterogeneous combustible media. *International Journal of Heat and Mass Transfer, 41(6-7)*, 1997, 881-897.

[6] Andrews P.L. BEHAVE: Fire behavior prediction and fuel modeling subsystem. (USDA Forest Service Report INT-194, Intermountain Research Station, Ogden, UT 84401, 1986).

[7] Finney M.A. FARSITE: Fire area simulator – model development and evaluation. *Res*. *Pap*. *RMRS-RP-4*, *Ogden*, *Utah*: *USDA*, *Forest Service*, Rocky Mountains Research Station, 1998.

[8] Linn R.R. and Harlow F.H. FIRETEC: A transport description of wildfire behavior. *Preprints of 2nd Symp. on Forest and Fire Meteorology*, *AMS 78th Annual Meeting*, 1998, 11-16.

[9] Balbi, J. H., Santoni, P. A. and Dupuy, J.L. Dynamic modeling of fire spread across a fuel bed. *International Journal of Wildland Fire*, 2000 (*in press*).

[10] Santoni, P. A., Balbi, J. H. and Dupuy, J.L. Dynamic modelling of upslope fire growth. *International Journal of Wildland Fire*, 2000 (*in press*).

[11] Morandini, F., Santoni, P.A., and Balbi, J.H. Analogy between wind and slope effects on fire spread across a fuel bed – Modelling and validations. *3rd Int. Sem. on Fire and explosion hazards*, 2000.

[12] Simeoni, A., Santoni, P.A., Larini, M., and Balbi, J.H. Proposal for Theoretical Improvement of Semi-Physical Forest Fire Spread Models Thanks to a Multiphase Approach: Application to a Fire Spread Model Across a Fuel Bed. *Combustion Science and Technology*, 2000 (*in press*).

[13] Patankar, S.V. Numerical Heat Transfer and Fluid Flow. (Hemisphere Publishing Corporation, 1980).

[14] Simeoni, A., Santoni P.A. and Balbi J.H. (1998) Optimal discretization of a continuous fire spread model. *III Int. Conf. on Fire Research, 1*, 311-323.

[15] Dupuy J.L. Slope and fuel load effects on fire behaviour: Laboratory experiments in pine needles fuel beds. *International Journal of Wildland Fire*, *5(3)*, 1995, 153.

[16] Mendes-Lopes, J.M., Ventura, J.M., and Amaral, J.M. Rate of spread and flame characteristics in a bed of pine needles. *III Int. Conf. on Fire Research, 1*, 1998, 497-511.

[17] Ventura, J. M., Mendes-Lopes, J. M. and Ripado, L.M. Temperature-time curves in fire propagating in beds of pine needles. *III Int. Conf. on Fire Research, 1*, 1998, 699-711.

[18] Den Breejen, E., Roos, M., Schutte, K., De Vries, J. S. and Winkel, H. Infrared measurements of energy release and flame temperatures of forest fires. *III Int. Conf. on Fire Research, 1*, 1998, 517-532.

Nomenclature

A heat exchanges matrix

C sources vector

C_p specific heat at constant pressure

e total energy

$\vec{g}$ acceleration due to gravity

G calculation point gain

k reduced heat transfer coefficient

k_v reduced advection coefficient

k_v^* constant in the k_v expression

K thermal diffusivity

L heat of vaporisation

m surface thermal mass

$\dot{M}$ mass flux

n cell number

p_0 empirical constant

P reduced radiative coefficient

q heat flux

Q reduced combustion enthalpy

R radiant flux

t time

T temperature

$\vec{V}$ velocity

$\vec{V}_\infty$ maximal wind velocity

x,y,z co-ordinate in space

Y mass fraction

Greek symbols

α volume fraction

γ combustion time constant

Γ rate of production at the solid / gas interface

δ thickness of the fuel layer

ΔH reaction enthalpy of solid phases

Δt time step

Δx mesh size

θ angle located between the normal of the front and the direction of spread

Θ temperature vector

$\overline{\overline{\pi}}$ stress tensor in the gas

$\vec{\Pi}$ stresses at the solid / gas interface

ρ density

σ surface mass

ϕ flame tilt angle

$\dot{\omega}$ species mass rate of production

$\vec{\nabla}_s$ surface divergence vector

Diacriticals

$[\ ]$ source term

Subscripts

a ambient

bu burning area

do burned area

eq medium equivalent to the litter

g gaseous phase

gk interface exchanges

i cell number along the *x* axis

j cell number along the *y* axis

ig ignition

k solid phase

s surface component of a vector

z vertical co-ordinate

up unburned area

0 initial condition

superscripts

i chemical species *i*

pr gaseous products

surf surface regression

δ value at the top of the bed

Biographies

Jacques-Henri Balbi is the President of the University of Corsica (France). He is also a Professor in physics and Director of the "Sciences Pour l'Environnement" department – UMR CNRS laboratory No. 6134, which associates the scientists of the University of Corsica with the CNRS. He has initiated the research on fire spread modelling in this University with P.A. Santoni who has began his Ph.D. thesis under his management.

Paul-Antoine Santoni is the Manager of the team « Feu de forêt » which works on fire spread modelling. He is an Assistant-Professor at the University of Corsica. He is engineer in electronic and doctor in energetic. His work is mainly concerned with the fire spread

modelling, but he also manages experiments and simulations to validate his models. He works currently with two Ph.D. students in the frame of fire spread models improvement.

Albert Simeoni is an Assistant-Professor at the University of Corsica. He is engineer and doctor in energetic. His work is mainly concerned with the fire spread modelling and particularly the reduction of complete physical models to create simple models to be included in fire simulators.